Dual-stimuli responsive liposomes using pH- and temperature-sensitive polymers for controlled transdermal delivery

Dual-stimuli responsive liposomes using pH- and temperature-sensitive polymers for controlled transdermal delivery

Naoko Yamazaki[1,3], Takumi Sugimoto[3], Mitsuhiro Fukushima[2], Ryoma Teranishi[3], Aki Kotaka[1], Chiharu Shinde[1], Takayuki Kumei[1], Yasushi Sumida[1], Yuki Munekata[2], Keiichi Maruyama[2], Eiji Yuba[3,*], Atsushi Harada[3], and Kenji Kono[3]

[1]Research Institute, Fancl Corporation, 12-13 Kamishinano, Totsuka-ku, Yokohama, Kanagawa, Japan; [2]Oleo & Speciality Chemicals Research Laboratory, NOF Corporation, Amagasaki, Hyogo 660-0095, Japan; [3]Department of Applied Chemistry, Graduate School of Engineering, Osaka Prefecture University, 1-1 Gakuen-cho, Naka-ku, Sakai, Osaka 599-8531, Japan

***Corresponding author: Eiji Yuba**

Department of Applied Chemistry, Graduate School of Engineering,
Osaka Prefecture University, 1-1 Gakuen-cho, Nakaku, Sakai, Osaka 599-8531, Japan
Tel.: +81-722-54-9913; Fax: +81-722-54-9913; yuba@chem.osakafu-u.ac.jp

Keywords:

19 liposome / temperature-sensitive / pH-sensitive / transdermal delivery / cosmetics

20

21 **ABSTRACT**

22 Recent development in transdermal drug delivery systems has led to improvement of
23 systemic and local efficacies. In the cosmetics field, liposomes have long been used as
24 a container of cosmetic agents for their protection. Considering that these agents
25 should be released from the liposomes at appropriate sites during their penetration into
26 the skin, the use of skin environment-sensitive liposomes for transdermal penetration
27 is beneficial for improving cosmetics efficacy. For this study, we prepared novel
28 functional liposomes modified with methacrylate-based copolymers
29 poly(MD-co-MAA-co-LT)s, which have sensitivity to both temperature and pH.
30 Poly(MD-co-MAA-co-LT)s changed their water-solubility in response to both pH and
31 temperature. Poly(MD-co-MAA-co-LT)-modified liposomes showed content release
32 in conditions with acidic pH and temperatures higher than 35 °C, which correspond to
33 endosome/lysosome environments of the melanocytes at the stratum basale of the skin.
34 Polymer-modified liposomes were taken up efficiently by a murine melanoma cell line,
35 B16-F10 cells, which delivered their contents into endosomes and cytosol.
36 Polymer-modified liposomes could penetrate into deep layers of skin models and
37 reached to stratum basale. Results demonstrate that

poly(MD-co-MAA-co-LT)-modified liposomes are promising as a system for delivering cosmetic agents to melanocytes.

1. Introduction

In the medical field, transdermal drug delivery systems (TDDSs) have been studied intensively for drug administration methods instead of intravenously injected drugs and orally administered drugs. In the field of cosmetics, TDDS is an attractive method to deliver active agents to the skin interior and to improve skin surface conditions for anti-aging effects.[1] Skin is an important tissue separating the exterior environment and the body, acting as a protective barrier against harmful environmental effects. The skin surface takes a block mortar structure composed of well-ordered keratinocytes resembling a brick wall, with intercellular lipids (stratum corneum) as the mortar.[2] Intercellular lipids in the stratum corneum present a barrier preventing the invasion of various allergens and bacteria. Moreover, they control trans-epidermal water loss from the skin.[3] The epidermis, basement membrane, and dermis layer underlie the stratum corneum. When UV-A and UV-B are irradiated to skin or reactive oxygen species are produced in the skin, melanocytes in the stratum basale produce melanin granules to protect the skin from damage.[4] Therefore, the delivery of antioxidants or UV-protective agents to melanocytes is regarded as an effective means of protection against the production of melanin and freckles.[5] Because of skin barrier functions, it is

58 difficult to penetrate the dermis and insert active agents deep into skin tissues such as
59 the epidermis.[6]

60 To date, TDDSs of two types have been studied to improve the penetration of active
61 agents into skin: nanocarrier-based methods, physical techniques such as iontophoresis,
62 electroporation, and the use of microneedles and pasting agents.[1, 7, 8] Actually,
63 iontophoresis and electroporation are used to promote the penetration of water-soluble
64 molecules by a difference of voltage produced by electric fields. However, these
65 methods are inapplicable with water-insoluble drugs. The micrometer-sized needles
66 (microneedles) penetrate directly into the corner layer and introduce drug molecules
67 into the dermis. However, adjustment is difficult because the penetration depth
68 depends on the angle and applied strength. For pasting agents or patches, it is difficult
69 to find a balance between drug stability, skin acidity, and transdermal delivery
70 functions.

71 Nanocarrier-based transdermal delivery systems such as polymer micelles, nanogels,
72 and liposomes have also been studied intensively.[9–26] Among them, liposome-based
73 TDDSs are more practical than other delivery systems because of their capability to
74 encapsulate both water-soluble and water-insoluble drugs, to control the size and
75 surface charges, and to introduce various functions.[27–35] Many studies have suggested

that liposomes of various types can penetrate into the skin tissues and deliver their cargo to cells existing on the basement membrane.[3, 4, 17-21, 32-39] In addition, because liposomes comprise phospholipids, which are the same components as those in skin tissues, liposomes are regarded as showing few stimuli and little toxicity to skin. Actually, some liposomes have been used as additives in commercially available cosmetics.[17] In such applications, liposomes are used merely as carriers. Their drug release control has not been well-studied. For more precise delivery of drugs to target cells (melanocytes) existing at the stratum basale, liposomes having skin environmental stimuli-responsive properties are desired.

Deep sites of the skin have higher temperatures than those outside and the skin surface (e.g., skin surface temperature is about 30°C, whereas the temperature of deep skin sites is 37 °C when the environmental temperature is 25 °C)[40]. Furthermore, although skin tissues are mildly acidic to neutral pH, after internalization of liposomes via endocytosis, liposomes are located in endosomes and lysosomes with acidic pH.[41–45] Therefore, dual-stimuli (temperature and pH)-sensitive liposomes are useful for the precise delivery of drugs to the interior of melanocytes deep inside skin tissues. Stimuli-sensitive liposomes are generally prepared using two methods: liposomes containing pH-sensitive or temperature-sensitive lipids, and stable liposomes modified

94 with pH-sensitive or temperature-sensitive polymers.[46–55] From the perspective of
95 liposome stability, stimuli-sensitive polymer-modified liposomes are beneficial.
96 For this study, pH-sensitive and temperature-sensitive liposomes were prepared
97 using liposomes modified with pH-sensitive and temperature-sensitive polymers (Fig.
98 1). Methacrylate-based monomers of three kinds, methoxy diethyleneglycol
99 methacrylate (MD), methacrylic acid (MAA), and lauroxy tetraethyleneglycol
100 methacrylate (LT), were used, respectively, for temperature-sensitivity, pH-sensitivity
101 and anchoring. Their random copolymers (poly(MD-MAA-LT)) were prepared using a
102 free radical initiator. These copolymer-modified liposomes are expected to deliver the
103 active agents to melanocytes and to release drugs inside of these cells responding to
104 endosomal acidic pH and high temperature at the stratum basale (Fig. 1). Here, the
105 synthesis of dual stimuli-sensitive polymers was examined along with characterization
106 of polymers, drug-release performance of polymer-modified liposomes at
107 skin-mimetic environments, intracellular delivery of model drugs to melanocytes and
108 the penetration of liposomes using human 3-dimensional cultured epidermal model.
109

110 **2. Experimental methods**

111 *2.1. Materials*

112 Methoxy diethylene glycol methacrylate (MD, BLEMMER® PME-100), lauroxy
113 tetraethylene glycol methacrylate (LT, BLEMMER® PLE-200), and dipropyl
114 peroxydicarbonate (PEROYL® NPP) were obtained from NOF Corp. (Tokyo, Japan).
115 Methacrylic acid (MAA) was obtained from Kuraray Co. Ltd. (Tokyo, Japan).
116 Non-hydrogenated soy bean PC (SPC) was provided by Lipoid GmbH (Ludwigshafen,
117 Germany). Calcein was from Sigma-Aldrich Corp. (St. Louis, USA). Lissamine
118 rhodamine B-sulfonylphosphatidylethanolamine (Rh-PE) was purchased from Avanti
119 Polar Lipids Inc. (Birmingham, AL, USA). Triton X was obtained from Tokyo
120 Chemical Industry Co., Ltd. (Tokyo, Japan). Test-Wako-C was obtained from Wako
121 Pure Chemical Inds. Ltd. (Osaka, Japan).

122 *2.2. Synthesis of Poly(MD-co-MAA-co-LT)s*

123 Poly(MD-co-MAA-co-LT)s were synthesized by radical copolymerization of MD,
124 MAA, and LT using dipropyl peroxydicarbonate as an initiator (Scheme 1). For
125 synthesis of MD-MAA_{40}-LT, MD (64.1 g), MAA (21.6 g), LT (14.4 g), and dipropyl
126 peroxydicarbonate (1.94 g) were added dropwise into freshly distilled isopropanol
127 (100 g) under N_2 atmosphere and were kept at 60 °C for 2 h. Then the solution was
128 heated at 80 °C for 1 h under N_2 atmosphere. The obtained polymers were recovered
129 by removal of solvents under the vacuum. The yield was 99.8 g (97.8%). Other

130 polymers were synthesized using the same procedure at different feeds, as shown in
131 Table 1. The number-average molecular weight (*Mn*), the weight-average molecular
132 weight (*Mw*), and polydispersity index (*Mw/Mn*) of the copolymers were evaluated
133 using gel-permeation chromatography on a system equipped with a column (Shodex
134 LF-804; Showa Denko K.K., Tokyo, Japan) with THF as an eluent. Polystyrene was
135 used as a standard. Molar ratio of MD/LT and MAA units in the copolymers were
136 estimated using ^{1}H NMR (JNM-AL-400; JEOL, Tokyo, Japan) and acid value test as
137 described in JIS K 0070-1992, respectively. Briefly, titration of polymer dissolved in
138 methanol (20 mg/mL) using 0.1 M KOH (ethanol/water = 95/5, v/v) was performed
139 and the wt% of MAA units in the copolymer was calculated compared with theoretical
140 acid value of poly(methacrylic acid). Molar ratio of MD units and LT units was
141 calculated from the peak for alkyl group in LT units (δ: 1.2~1.4 (br, 20H,
142 -$CH_2C_{10}H_{20}CH_3$) and the peak for methoxy groups in MD units (δ: 3~3.5 (br, 3H,
143 -OCH_3). This molar ratio was once converted to wt% and then, wt% of MAA, MD and
144 LT units was calculated. Finally, the wt% values were divided by the unit molecular
145 weights and converted to the unit molar ratio.

146 *2.3. Cloud Point Determination*

147 The turbidity of the copolymer PBS solution (10 mg/mL) as a function of
148 temperature was measured at 500 nm using a spectrophotometer (V-560; Jasco Corp.,
149 Tokyo, Japan) equipped with a Peltier type thermostatic cell holder, coupled with an
150 ETC-505T controller. Temperature was raised at 2 °C/min. Cloud points were taken as
151 the initial break points in the resulting transmittance versus temperature curves.

152 *2.4. Determination of the Transition Temperature of Copolymers by DSC*

153 Thermograms of copolymers dissolved in 10 mM phosphate and 140 mM NaCl
154 were recorded by NANO DSC (TA Instruments, New Castle, DE, USA). The
155 copolymer solutions were placed in a sample cell and were analyzed at a heating rate
156 of 1.0 °C/min.

157 *2.5 Preparation of Calcein-Loaded Liposomes*

158 Given amounts of chloroform solution of SPC (23 mg) and copolymer (1 mg) were
159 added to a flask. Then the solvent was evaporated. The obtained thin film was dried
160 further under vacuum overnight and was dispersed in 2 mL of aqueous calcein solution
161 (63 mM, pH 7.4). The liposome suspension was extruded through a polycarbonate
162 membrane with pore diameter of 100 nm in an ice-cooled water bath. The free calcein
163 and free copolymer were removed using Sephadex G-50 column (GE Healthcare UK
164 Ltd., Buckinghamshire, England) at 4 °C in a 10 mM phosphate and 137 mM NaCl

165 solution at pH 9.0. The lipid concentration was ascertained (Test-Wako-C; Wako Pure
166 Chemical Inds. Ltd., Osaka, Japan). The calcein-loaded liposomes were kept at 5 °C
167 until measurement. The liposome size was evaluated using dynamic light scattering
168 (ELS-8000 and ELS-Z 1000; Otsuka Electronics Co. Ltd., Tokyo, Japan) in PBS(-),
169 pH 7.4, at 25 °C. Transmission electron microscopic (TEM) analysis for the liposomes
170 stained by phosphotungstic acid solution was performed using JEM-2000FEX II
171 (JEOL Ltd., Tokyo, Japan) with carbon-coated copper grids.

172 *2.6. Calcein Release from Liposomes*

173 Liposome suspension was added to PBS(-) (4.0 mL) at various pH (pH4.0–7.4) and
174 temperatures (25–70 °C). Calcein fluorescence at 520 nm with excitation at 490 nm
175 was measured using a spectrophotofluorimeter (Spectra Max Gemini EM; Molecular
176 Devices Corp., Montana, USA). The percent release of calcein from liposome was
177 defined as

178 $$\%\text{Release} = (F - F_0)/(F_{100} - F_0) \times 100$$

179 where F_0 and F respectively denote the initial and intermediary fluorescence
180 intensities of the liposome suspension at 5 °C. F_{100} is the fluorescence intensity of the
181 liposome suspension after the addition of Triton X-100 (final concentration, 0.2 wt%).
182 F_{100} of liposomes (lipid concentration: 20 μM) after addition of Triton-X100 (final

concentration: 0.2 wt%) were 3195 ± 179 (a. u.) for unmodified liposome, 2725 ± 80 (a. u.) for liposomes modified with MD-MAA_0-LT, 2499 ± 282 (a. u.) for MD-MAA_{20}-LT, 2056 ± 39 (a. u.) for MD-MAA_{30}-LT, and 1913 ± 75 (a. u.) for MD-MAA_{40}-LT.

2.7. Confocal Laser Scanning Microscopic Observation and Flow Cytometry

First, 2.0×10^5 of B16-F10 melanoma cells obtained from Tohoku University (Sendai, Japan) were grown in DMEM containing 10% FBS for 24 h in humidified atmosphere containing 5% CO_2 at 37 °C. 0.2 mol% of The rhodamine-PE-labeled and calcein-loaded liposomes modified with or without MD-MAA_{40}-LT copolymer were added (0.5 mM lipid concentration) to cells in serum-free DMEM and were incubated for 3 h at 37 °C. The cells were washed with PBS(+) and were observed using confocal laser scanning microscopy (LSM 5 Exciter; Carl Zeiss Inc., Oberkochen, Germany) and flow cytometers (CytoFlex; Beckman Coulter Inc., Fullerton, CA, USA).[55–58]

2.8. Evaluation of liposomes penetration in skin models

3D skin models (LabCyte EPI-MODEL, Japan Tissue Engineering Co., Ltd., Aichi, Japan) were used for the evaluation of liposome penetration. 3D skin models were treated with calcein solution (25.2 μM) or 0.2 mol% Rh-PE-labeled liposomes

containing calcein (lipid and calcein concentrations were 1 mM and 25.2 μM, respectively) for 24 h in PBS. After removal of supernatant, 3D skin models were frozen immediately after embedding in Tissue-Tek O.C.T. Compound (Sakura Finetek Japan Co., Ltd., Tokyo, Japan). Skin models were sectioned 10 μm slices and mounted on glass slides by New Histo. Science Laboratory Co., LTd. (Tokyo, Japan). Confocal laser scanning microscopic analysis of these slides was performed using LSM 5 Exciter (Carl Zeiss Inc., Oberkochen, Germany).

3. Results and Discussion

3.1 *Characterization of pH-sensitive and Thermo-sensitive Polymers*

Poly(MD-co-MAA-co-LT)s having carboxyl units, oligo(ethylene glycol) units and hydrophobic units were synthesized by radical copolymerization of MD, MAA, and LT. The compositions and molecular weight of obtained polymers were evaluated, respectively, using NMR and GPC (Table 1). Results show that compositions of poly(MD-co-MAA-co-LT)s were almost identical to the feed ratio of respective monomers. By changing the feed ratios of monomers, poly(MD-co-MAA-co-LT)s having various MD/MAA unit ratios and 5% of LT units were synthesized. Molecular

218 weights of these polymers were 5,000–24,000. The molecular weight distributions
219 were high, reflecting radical polymerization.
220 Because poly(MD-co-MAA-co-LT)s have both carboxyl groups and oligo(ethylene
221 glycol) groups, they are expected to respond to both pH and temperature. Therefore,
222 pH-sensitive and temperature-sensitive properties of the poly(MD-co-MAA-co-LT)s
223 were examined using detection of phase separation of the polymer's aqueous solutions.
224 Figures 2a–2d respectively portray the optical transmittance of the MD-MAA_0-LT,
225 MD-MAA_{30}-LT, MD-MAA_{40}-LT, and MD-MAA_{45}-LT aqueous solutions at various
226 pH as a function of temperature. The cloud points of polymer solution, defined as the
227 temperature at the transmittance, began to decrease drastically.[59] As presented in Fig.
228 2a, the solution of poly(MD-MAA_0-LT) suddenly became turbid at temperatures
229 higher than 13 °C, which indicates that this polymer lost water-solubility because of
230 dehydration of oligo(ethylene glycol) units responding to the temperature increase.
231 Poly(MD-MAA_0-LT) showed the same cloud points irrespective of the solution pH
232 (Fig. 2a). Poly(MD-MAA_0-LT) has no protonation groups. Therefore, this polymer
233 shows only temperature sensitivity. In the case of poly(MD-MAA_{30}-LT), the solution
234 of this polymer at pH 7.4 was transparent at 10–70 °C. However, at acidic pH,
235 poly(MD-MAA_{30}-LT) showed cloud points (Fig. 2b). The carboxyl groups of MAA

236 unit are deprotonated at neutral pH. For that reason, the polymer aggregation might be
237 inhibited by electro-repulsion of the deprotonated carboxyl groups even after
238 dehydration of MD units at high temperatures. After protonation of carboxyl groups of
239 MAA unit with pH decreasing, polymers became water-insoluble. Therefore, this
240 polymer is sensitive to both pH and temperature. Poly(MD-MAA_{40}-LT) and
241 poly(MD-MAA_{45}-LT) showed the same tendency with poly(MD-MAA_{30}-LT) (Figs. 2c
242 and 2d). Cloud points of these polymers increased concomitantly with increasing
243 MAA contents at the same pH, which indicates that higher temperatures are necessary
244 for the aggregation of polymers with higher contents of deprotonated carboxyl groups
245 on the polymer chains. The pH and MAA content dependences of cloud points for
246 these polymers are presented in Figure 3.
247 To evaluate correlation between the phase separation of these polymers and the
248 dehydration of side chain units, DSC measurements for the polymers were examined.
249 Figure 4 presents thermograms for respective polymers. Their cloud points,
250 endothermic peak, and calculated ΔH are presented in Table 2. The endothermic peaks
251 for respective polymers mostly agreed with the cloud point measured by turbidity
252 measurements, suggesting that the endotherms are derived from dehydration upon the
253 conformational transition of the polymer chains. Compared with poly(MD-MAA_0-LT),

254 ΔH values for poly(MD-MAA_{20}-LT), poly(MD-MAA_{30}-LT), and
255 poly(MD-MAA_{40}-LT) were quite low (Table 2). Assuming that dehydration mainly
256 takes place at oligo(ethylene glycol) units, ΔH values per MD units were calculated
257 (Table 2). Poly(MD-MAA_0-LT) showed ΔH values irrespective of pH, although
258 MAA-containing polymers showed quite low ΔH values per MD units. These results
259 indicate that the protonated carboxyl groups might form hydrogen bonds with
260 oligo(ethylene glycol) units and promote polymer aggregation. Therefore, these
261 polymers might show phase separation even at low dehydration of MD units.

262 *3.2 Characterization of Dual Stimuli-Responsive Behaviors of Polymer-Modified*
263 *Liposomes*

264 Next, pH-sensitivity and temperature-sensitivity of liposomes modified with
265 copolymers were evaluated. Each polymer has LT units as hydrophobic groups, which
266 enables fixing of these polymers to a liposomal membrane via hydrophobic
267 interactions. Table 3 shows that the diameters of SPC-based liposomes modified with
268 these copolymers at a weight ratio of 1/23 (polymer/lipid) were almost identical to
269 those of polymer-unmodified liposomes. Figure 5 shows the TEM images of
270 liposomes. Typical spherical and vesicular structures with size of around 100 nm for
271 liposomes were observed. A fluorescence dye, calcein, was encapsulated to liposomes.

Their content-release properties were evaluated. Comparison of calcein fluorescence intensities after liposome disruption revealed that MAA-containing copolymer-modified liposomes had somewhat lower calcein encapsulation than the unmodified or MAA-free copolymer-modified liposomes (see Experimental section). Probably, negatively charged calcein molecules can be excluded from the liposome surface spaces of the rumen through electrostatic and steric repulsive forces of copolymers. Figure 6a depicts the pH-dependence of calcein release at 25 °C and 35 °C, which corresponds to skin temperature. Polymer-unmodified liposomes showed no content release at any pH. In addition, poly(MD-MAA_0-LT)-modified liposomes show no content release at any pH region or at 25 °C and 35 °C, although poly(MD-MAA_0-LT) became hydrophobic at these temperatures (Fig. 2a). In contrast, MAA unit-containing polymer-modified liposomes were stable at neutral pH, but exhibited content release at weakly acidic pH. These results indicate that carboxyl groups on the polymer chain are important to induce liposomal membrane destabilization. Poly(carboxylic acid) derivatives are known to form hydrogen bonds with phosphate groups on liposomal membrane and induce membrane lysis or destabilization.[46, 57, 61] Although poly(MD-MAA_0-LT) became hydrophobic at 25 °C and 35 °C (Fig. 2a), polymer chains might be unable to interact with liposome

290 efficiently because of the lack of hydrogen bond formation. In contrast, MAA
291 unit-containing polymers might form hydrogen bonds with a liposomal membrane and
292 might be able to approach to liposome surface. Subsequently, they destabilize *via*
293 hydrophobic interaction. Especially, poly(MD-MAA_{40}-LT)-modified liposomes
294 showed no content release at 25 °C and pH 7.4, but promoted release at 35 °C and
295 below at pH 6.5. According to turbidity measurements, poly(MD-MAA_{40}-LT) showed
296 no transmittance decrease at pH 7.4–5.5 and 35 °C (Fig. 2c), which indicates that
297 hydrophobization of poly(MD-MAA_{40}-LT) existing at the periphery of the liposome
298 surface might be promoted because of the hydrophobic environment of the lipid
299 membrane, resulting in efficient destabilization of liposomal membrane at 35 °C and
300 below at pH 6.5.
301 Temperature-sensitivity of polymer-modified liposomes was evaluated at pH 7.4
302 and 5.0 (Fig. 6b). At pH 7.4, no liposome showed any content release at any
303 temperature region after 10 min incubation. In contrast, at pH 5.0, polymer-modified
304 liposomes exhibited content release, especially at temperatures higher than 35 °C. In
305 addition, the extent of content release increased concomitantly with decreasing MAA
306 contents in copolymers. According to results of cloud point measurements,
307 copolymers with lower MAA contents have more hydrophobic properties, which

might induce more efficient membrane destabilization. Consequently, poly(MD-MAA-LT)-modified liposomes showed content release in response to both pH and temperature. Release behaviors are also controllable by changing the MAA contents of the copolymers. Especially, poly(MD-MAA_{40}-LT)-modified liposomes exhibited remarkable content release in conditions with acidic pH and temperatures higher than 35°C, which correspond to the temperature and the pH of a skin environment. The poly(MD-MAA_{45}-LT)-modified liposomes showed content release at temperatures higher than 50 °C. The poly(MD-MAA_{50}-LT)-modified liposomes showed low content release behavior. Their yield was low (data not shown). Therefore, poly(MD-MAA_{40}-LT)-modified liposomes were used for the following experiments.

3.3 Intracellular Behavior

Next, intracellular delivery performance of copolymer-modified liposomes was evaluated. Murine melanoma-derived B16F10 cells were used as model melanocytes. Rh-PE-labeled and calcein-loaded liposomes were applied to B16F10 cells. After 3 h, intracellular distribution of liposome and calcein was observed using confocal laser scanning microscopy (Fig. 7). As presented in Fig. 7A, cells treated with unmodified SPC liposomes displayed punctate fluorescence of Rh-PE, but calcein fluorescence was not observed from the same locations of Rh-PE, suggesting that the unmodified

326 liposomes were taken up by cells via endocytosis, but they retained calcein molecules
327 inside of liposomes. In contrast, cells treated with the poly(MD-MAA_{40}-LT)-modified
328 liposomes displayed strong fluorescence of both Rh-PE and calcein, indicating that
329 polymer-modified liposomes were taken up by melanocytes more efficiently than
330 unmodified liposomes and released calcein molecules from liposomes responding the
331 intracellular acidic pH and cultural temperature (37 °C).[61, 62] In addition, some green
332 fluorescence was observed at locations different from those showing red fluorescence.
333 Poly(MD-MAA_{40}-LT)-modified liposomes might destabilize not only their own
334 liposomal membranes but also endosomal membranes, resulting in cytoplasmic
335 delivery of contents. Cells treated with calcein solution showed much weaker green
336 fluorescence than polymer-modified liposomes did (Fig. 7C).
337 Next, flow cytometry was used to evaluate the delivery kinetics of liposomes and
338 calcein (Fig. 8). B16–F10 melanoma cells that had been treated with liposomes for 2 h
339 or 3 h and cellular fluorescence at varying times were measured. Unmodified liposome
340 and poly(MD-MAA_{40}-LT)-modified liposome-treated cells respectively showed
341 calcein and Rh-PE-derived fluorescence. The fluorescence increased concomitantly
342 with increased incubation time (Figs. 8c and 8d). Poly(MD-MAA_{40}-LT)-modified
343 liposomes showed higher fluorescence intensity than unmodified liposomes did,

344 reflecting the results of CLSM images (Figs. 8a and 8b). However, cells treated with
345 the calcein solution displayed very low fluorescence of calcein. These results
346 demonstrate that calcein molecules were released efficiently from
347 Poly(MD-MAA_{40}-LT)-modified liposomes by pH and temperature sensitivity of
348 MD-MAA_{40}-LT polymer.

349 *3.4. Penetration of liposomes in skin models*

350 Finally, the skin penetration experiments of liposomes were examined using 3D
351 skin models (LabCyte EPI MODEL), which are commonly used for the evaluation of
352 drug penetration in the cosmetic field.[63] Figure 9 shows confocal laser scanning
353 microscopic images of 3D skin models treated with PBS, calcein solution,
354 calcein-loaded unmodified liposomes and MD-MAA_{40}-LT-modified liposomes.
355 Liposomes were fluorescently labeled with 0.2 mol% of rhodamine-lipids. As shown
356 in Fig. 9b, calcein solution hardly penetrated the skin model and quite weak green
357 fluorescence was observed from the surface, which corresponds to stratum corneum.
358 In contrast, strong green and red fluorescence was observed from the surface of skin
359 models treated with liposomes. MD-MAA_{40}-LT-modified liposomes showed much
360 higher fluorescence than that of unmodified liposomes, which might reflect the high
361 cellular association of MD-MAA_{40}-LT-modified liposomes in Figure 8. In addition,

362 fluorescence derived from liposome and calcein diffused to underlayers, which
363 correspond to stratum granulosum and stratum spinosum. Green and red fluorescence
364 was also detected from stratum basale in the both cases of liposome-treated skin
365 models. These results indicate that most of liposomes absorbed on the skin surface but
366 a part of liposomes diffused to the underlayers and reached to stratum basale. In
367 addition, both calcein and rhodamine fluorescence was detected from stratum basale,
368 which might suggest that liposomes retained the calcein molecules during the
369 penetration into stratum basale. Combined with the results in Figures 7-9,
370 MD-MAA_{40}-LT-modified liposomes might efficiently absorb to surface of skin and a
371 part of liposomes penetrate into stratum basale and be taken up by melanocytes. Then,
372 liposomes might release drugs responding to both high temperature at stratum basale
373 and low pH in endosomes of melanocytes.
374
375 **4. Conclusion**
376 For this study, a dual stimuli-sensitive polymer was newly developed:
377 poly(MD-co-MAA-co-LT). Liposomes were modified with copolymers to produce
378 functional DDS with destabilization that might be triggered by a combination of acidic
379 pH signals and temperature signals. Poly(MD-co-MAA-co-LT) changed their water

solubility depending on pH and temperature. Contents released from the copolymer-modified liposomes were enhanced in weakly acidic pH and body-temperature conditions, corresponding to a skin environment. Therefore, these liposomes have potential usefulness for the selective delivery of antioxidants or UV-protective agents to melanocytes existing in deep skin tissues, which provides highly protective effects against the production of melanin and freckles. These skin-environment-responsive liposomes can be exploited not only for use in cosmetics delivery systems but also for transdermal drug delivery systems.

Acknowledgment

This work was supported by a Grant-in-aid for Scientific Research from the Ministry of Education, Science, Sports, and Culture in Japan (26242049).

Author Contribution

KK conceived the idea and supervised the work. MF, YM and KM synthesized the polymers and performed NMR and GPC analyses. NY and TS performed the turbidity and DSC measurements of polymers and they prepared the polymer-modified liposomes and performed the characterization of liposomes and the cellular

398 experiments. NY and RT performed TEM measurements of liposomes. YS, TK, AK
399 and CH performed the evaluation of data. The manuscript was written through
400 contributions from KK, AH, EY and NY. All authors have given approval to the final
401 version of the manuscript.
402

403 **References**

404 1. B. W. Barry, *Eur. J. Pharm. Sci*., 2007, **14**, 101.

405 2. P. M. Elias, *J. Invest. Dermatol.,* 1983, **80,** 44.

406 3. K. Kikuchi, H. Kobayashi, T. Hirano, A. Ito, H. Takahashi, and H. Tagami,

407 *Dermatology*, 2003, **207**, 269.

408 4. Y. Shindo, E. Witt, L. Packer, and D. Han., *J. Invest. Dermatol*., 1993, **100**, 260.

409 5. Y. Shindo, E. Witt, D. Han, and L. Packer, *J. Invest. Dermatol*., 1994, **102**, 470.

410 6. D. Nava, *Cosmetics & Toiletries*, 2005, **120**, 67.

411 7. S. A. Burton, C. Y. Ng, R. Simmers, C. Moeckly, D. Brandwein, T. Gilbert, N.

412 Johnson, K. Brown, T Alston, G. Prochnow, K. Siebenaler, and K. Hansen., *Pharm.*

413 *Res*., 2011, **28**, 31.

414 8. V. Damme, F.Oosterhuis-Kafeja, M. Van der Wielen, Y. Almagor, O. Sharon, and

415 Y. Levin, *Vaccine,* 2009, **14**, 454.

416 9. N. Nishiyama, Y. Morimoto, W. D. Jang, and K. Kataoka, *Adv. Drug Deliv. Rev.*,

417 2009, **61**, 327.

418 10. E. Mahmoud, and L. Karen, *Chem. Soc. Rev.*, 2012, **41**, 2545.

419 11. S. Punit, D. Pinaki, P. Apurva, and S. Mandip, *Biomaterials*, 2012, **33**, 1607.

12. G. S. L. Singka, N. A. Samah, M. H. Zulfakar, A.Yurdasiperb, and C. M. Heard, *Eur. J. Pharm. Biopharm.,* 2012, **2**, 275.

13. B. W. Barry, *J. Control. Release,* 1987, **6**, 85.

14. H. E. Junginger, *Cosmetics & Toiletries,* 1991, **106**, 45.

15. G. M. E. Maghraby, B. W. Barry, and A. C. Williams, Eur. *J. Pharm. Sci*., 2008, **34**, 203.

16. D. D. Verma, S. Verma, G. Blume, and A. Fahr, *Eur. J. Immunol*., 2003, **55**, 258.

17. G. Cevc, G. Blume, A. Schätzleina, D. Gebauera, and A. Paula, *Adv. Drug Deliv. Rev.,* 1996, **18**, 349.

18. K. Egbaria, C. Ramachandran, D. Kittayanond, and N. Weiner, *Antimicrob. Agents Chemother.,* 1990, **34**, 107.

19. G. Cevc, A. Schätzlein, and H. Richardsen, *Biochim. Biophys. Acta,* 2002, **1564**, 21.

20. G. Cevc, and D. Gebauer. *Biophys. J*., 2003, **84**, 1010.

21. G. Cevc, D. Gebauer. J. Stieber, A. Schätzlein, and G. Blume, *Biochim. Biophys. Acta,* 1998, **1368**, 201.

22. Y. Yokomizo, *Int. J. Pharm.,* 1997, **147**, 219.

23. J. Lasch, R. Laub, and W. Wohlrab, *J. Control. Release,* 1996, **38**, 267.

438 24. N. Yamazaki, T. Kumei, C. Shinde, and Y. Sumida, *J. Soc. Cosmet. Chem. Jpn*.,
439 2016, **50**, 25.
440 25. J. Plessis, C. Ramachandran, N. Weiner, and D.G. Müller, *Int. J. Pharm*., 1994,
441 **103**, 277.
442 26. P. L. Honeywell-Nguyen, A. M. de Graaff, H. W. Wouter Groenink, and J. A.
443 Bouwstra, *Biochim. Biophys. Acta,* 2002, **1573**, 130.
444 27. D. D. Verma, S. Verma, G. Blume, and A. Fahr, *Eur. J. Pharm.,* 2003, **258**, 141.
445 28. H. E. Hofland, R. van der Geest, H. E. Bodde, H. E. Junginger, and J. A. Bouwstra,
446 *Pharm. Res*., 1994, **11**, 659.
447 29. Y. Yokomizo, and H. Sagitani, *J. Control. Release,* 1996, **38**, 267.
448 30. N. Yamazaki, I. Hisamitsu, and Y. Sumida, *J. Soc. Cosmet. Chem. Jpn.,* 2009, **43**,
449 260.
450 31. D. B. Yarosh, *Photodermatol. Photoimmunol. Photomed.*, 2001, **17**, 203.
451 32. S. I. Park, E. O. Lee, H. M. Yang, C. W. Park, and J. D. Kim. *Colloids Surf. B*
452 *Biointerfaces*, 2013, **110**, 333.
453 33. Y. Wang, W. Sub, Q. Li, C. Li, H. Wang, Y. Li, Y. Caoa, J. Chang, and L. Zhang,
454 *Int. J. Pharm.*, 2013, **441**, 748.
455 34. W. Zhou, W. Liu, L. Zou, W. Liu, C. Liu, R. Liang, and J. Chen, *Colloids Surf. B*

456 *Biointerfaces*, 2014, **117**, 330.

457 35. S. Jeon, C. Y. Yoo, and S. N. Park, *Colloids Surf. B Biointerfaces*, 2015, **129**, 7.

458 36. M. Foldvari, A. Gesztes, and M. Mezei, *J. Microencapsul.*, 1990, **7**, 479.

459 37. M. Fresta, and G. Puglisi, *J. Drug Target*, 1996, **4**, 95.

460 38. C. Valenta, and M. Janisch, *Int. J. Pharm.*, 2003, **258**, 133.

461 39. D. Verma, S. Verma, G. Blume, and A Fahr, *Int. J. Pharm.*, 2003, **258**, 141.

462 40. R. H. Fox, A. J. Solman, R. Isaacs, A. J. Fry, and I. C. MacDonald, *Clin. Sci.*, 1973,

463 **44**, 81.

464 41. N. Nakagawa, S. Sakai, M. Matsumoto, K. Yamada, M. Nagano, T. Yuki, Y.

465 Sumida, and H. Uchiwa, *J. Invest. Dermatol*., 2004, **122**, 755.

466 42. D. K. Harrison, V. A. Spence, J. Swanson Beck, J. G. Lowe, and W. F. Walker,

467 *Immunology,* 1986**, 59**, 497.

468 43. M. J. Behne, J. W. Meyer, K. M. Hanson, N. P. Barry, S. Murata, D. Crumrine, R.

469 W. Clegg, E. Gratton, W. M. Holleran, P. M. Elias, and T. M. Mauro., *J. Biol. Chem*.,

470 2002, **277**, 47399.

471 44. D. K. Harrison, and W. F. Walker, *J. Physiol*., 1979, **291**, 339.

472 45. T. Abe, J. Mayuzumi, N. Kikuchi, and S. Arai, *Chem. Pharm. Bull*., 1980, **28**, 387.

46. N. Sakaguchi, C. Kojima, A. Harada, and K. Kono, *Bioconj. Chem*., 2008, **19**, 1040.

47. K. Kono, A. Henmi, H. Yamashita, H. Hayashi, and T. Takagishi, *J. Control. Release,* 1999, **59**, 63.

48. H. Hayashi, K. Kono, and T. Takagishi, *Bioconj. Chem*., 1999, **10**, 412.

49. E. Yuba, Y. Kono, A. Harada, S. Yokoyama, M. Arai, K. Kubo, and K. Kono, *Biomaterials,* 2013, **34**, 5711.

50. K. Kono, T. Ozawa, T. Yoshida, F. Ozaki, Y. Ishizaka, K. Maruyama, C. Kojima, A. Harada, and S. Aoshima, *Biomaterials,* 2010, **31**, 7096.

51. E. Yuba, A. Harada, Y. Sakanishi, and K. Kono, *J. Control. Release,* 2011, **149**, 72.

52. M. Carafa, L. D. Marzio, C. Marianecci, B. Cinque, G. Lucania, K. Kajiwara, M. G. Cifone, and E. Santucci, *Eur. J. Pharm. Sci*., 2006, **28**, 385

53. I. M. Hafez, S. Ansell, and P. R. Cullis, *Biophy. J.*, 2000, **79**, 1438.

54. L. Qiu, Z. Li, M. Qiao, M. Long, M. Wang, X. Zhang, C. Tian, and D. Chen, *Acta Biomaterialia*, 2014, **10**, 2024.

55. V. A. Slepushkin, S. Simões, P. Dazin, M. S. Newman, L. S. Guo, M. C. P. de Lima, and N. Düzgüneş, *J. Biol. Chem*., 1997, **272**, 2382.

56. T. Kaiden, E. Yuba, A. Harada, Y. Sakanishi, and K. Kono, *Bioconj. Chem.*, 2011, **22**, 1909.

57. C. Kojima, K. Yoshimura, A. Harada, Y. Sakanishi, and K. Kono, *Bioconj. Chem.*, 2009, **20**, 1054.

58. K. F. Yu, W. Q. Zhang, L. M. Luo, P. Song, D. Li, R. Du, W. Ren, D. Huang, W. L. Lu, X. Zhang, and Q. Zhang, *Int. J. Nanomedicine,* 2013, **8**, 2473.

59. P. Reynier, D. Briane, A. Cao, N. Lievre, R. Naejus, P. Bissieres, J. L. Salzmann, and E. Taillandier, *J. Drug Target*, 2007, **10**, 557.

60. E. Koren, A. Apte, A. Jani, and V. P. Torchilin, *J. Control. Release,* 2012, **160**, 264.

61. K. Yoshino, A. Kadowaki, T. Takagishi, and K. Kono, *Bioconj. Chem.*, 2004, **15**, 1102.

62. T. Fujimura, S. Nakagawa, T. Ohtani, Y. Ito, and S. Aiba, *Eur. J. Immunology,* 2006, **36**, 3371.

63. T. Hikima, N. Kaneda, K. Matsuo, and K. Tojo, *Biol. Pharm. Bull.*, 2012, **35**, 362.

507 **Figure captions**

508 **Scheme 1.** Synthesis of poly(MD-MAA-LT)s.

509 **Figure 1.** pH-sensitive and temperature-sensitive polymer-modified liposomes as a

510 transdermal drug delivery system that responds to both high temperatures at the

511 epidermis and acidic pH at the endosome interior.

512 **Figure 2.** Transmittance of (a) MD-MAA_0-LT, (b) MD-MAA_{30}-LT, (c)

513 MD-MAA_{40}-LT, and (d) MD-MAA_{45}-LT copolymer solution (10 mg/mL) at various

514 pH as a function of temperature.

515 **Figure 3.** Cloud points of poly(MD-co-MAA-co-LT)s as a function of MAA contents

516 at pH 5.0 (open squares), pH 5.5 (closed squares), pH 5.8 (open triangles), pH 6.0

517 (open circles), pH 6.5 (closed circles), and pH 7.4 (open diamonds).

518 **Figure 3.** Cloud points of poly(MD-co-MAA-co-LT)s as a function of MAA contents

519 at pH 5.0 (open squares), pH 5.5 (closed squares), pH 5.8 (open triangles), pH 6.0

520 (open circles), pH 6.5 (closed circles), and pH 7.4 (open diamonds).

521 **Figure 4.** Microcalorimetric endotherms for (a) MD-MAA_0-LT, (b) MD-MAA_{20}-LT,

522 (c) MD-MAA_{30}-LT, and (d) MD-MAA_{40}-LT suspended in 10 mM phosphate buffer

523 containing 140 mM NaCl at various pH (10 mg/mL). Samples were heated at

524 1 °C/min.

525 **Figure 5.** TEM images for unmodified liposomes and MD-MAA_{40}-LT-modified

526 liposomes. Scale bars represent 100 nm.

527 **Figure 6.** pH-dependence (a) and temperature-dependence (b) of calcein release from

528 liposomes modified with MD-MAA_0-LT (diamonds), MD-MAA_{20}-LT (circles),

529 MD-MAA_{30}-LT (triangles), MD-MAA_{40}-LT (squares), and without polymers (crosses).

530 (a) Release after 30 min-incubation at 25 °C (open symbols) and 35 °C (closed

531 symbols) are shown. (b) Release after 10 min-incubation at pH 7.4 (open symbols) and

532 pH 5.0 (closed symbols) are shown.

533 **Figure 7.** Confocal laser scanning microscopic images of B16-F10 cells treated with

534 calcein-loaded, Rh-PE-labeled liposomes modified without (a) or with (b)

535 MD-MAA_{40}-LT and calcein solution (c) for 3 h.

536 **Figure 8.** Rhodamine (a) and calcein (b) fluorescence intensity for B16-F10 cells

537 treated with liposomes without (gray lines) or with (black line) MD-MAA_{40}-LT for 3 h.

538 Cell autofluorescence was set under 10^4. Time courses of rhodamine (c) and calcein

539 (d) fluorescence intensity for B16–F10 cells treated with calcein-loaded,

540 Rh-PE-labeled liposomes without (circles), or with MD-MAA_{40}-LT (squares) or

541 calcein solution (triangles). Cells were treated with liposomes for 2 or 3 h and washed

542 with PBS. Then, cellular fluorescence intensity was measured. In addition, cellular

543 fluorescence intensity was measured after incubation in the culture medium for
544 another 2 h for the cells treated with liposomes for 3 h and washed with PBS.
545 **Figure 9.** Confocal laser scanning microscopic images of the section of 3D skin
546 models treated with PBS (a), calcein solution (b), unmodified liposomes (c) and
547 MD-MAA_{40}-LT-modified liposomes (d) for 24 h. Calcein was encapsulated to
548 liposomes and liposomes were labeled with 0.2 mol% Rh-PE. Lipid and calcein
549 concentrations were 1 mM and 25.2 μM, respectively. The regions indicated by white
550 dotted lines represent stratum basale in the skin models. Magnified images for red
551 squares in Rh-PE fluorescence images are shown in right panels.
552

553 **Table 1. Compositions and Molecular Weights of Polymers**

Polymer	In feed (mol/mol/mol)	MD	MAA	LT	M_n [b]	M_w [b]	*Mw/Mn*
MD-MAA_{20}	80.0/20.0/0	80.9	19.1	0.0	18,870	74,400	3.9
MD-MAA_0-LT	94.7/0/5.3	95.2	0.0	4.8	10,510	58,120	5.5
MD-MAA_{20}-LT	74.7/20.0/5.3	75.3	19.5	5.2	23,680	72,770	3.1
MD-MAA_{30}-LT	64.7/30.0/5.3	67.9	27.9	4.2	22,120	64,170	2.9
MD-MAA_{40}-LT	54.7/40.0/5.3	58.7	37.6	3.7	22,320	61,110	2.7
MD-MAA_{45}-LT	49.7/45.0/5.3	51.3	44.0	4.7	9,080	70,040	7.7
MD-MAA_{50}-LT	44.7/50.0/5.3	48.0	47.6	4.4	20,480	67,680	3.3

a Determined by ^{1}H-NMR.

b Determined by ^{1}H-NMR and GPC measurements.

MD : methoxy diethyleneglycol methacrylate

MAA : methacrylic acid

LT : lauroxy tetraethyleneglycol methacrylate

554

555

556 **Table 2. Cloud Points and DSC Analysis of Polymers**

polymer	pH	Cloud Point (℃)	DSC		
			Tmax [a](℃)	ΔH (J/g)	ΔH (KJ/unit mol MD)
MD-MAA_0-LT	7.4	13	14.8 ± 0.1	19.3 ± 0.3	4.1 ± 0.0
	6	13.4	14.4 ± 0.2	19.2 ± 0.3	4.1 ± 0.0
	5.5	13.2	14.5 ± 0.2	19.3 ± 0.3	4.1 ± 0.1
MD-MAA_{20}-LT	7.4	N.D [b]	N.D [b]	N.D [b]	N.D [b]
	6	28.7	28.6 ± 0.1	2.3 ± 0.1	0.5 ± 0.0
	5.5	16.1	16.4 ± 0.2	6.0 ± 0.4	1.5 ± 0.1
MD-MAA30-LT	7.4	N.D [b]	N.D [b]	N.D [b]	N.D [b]
	6	44.1	35.3 ± 0.1	1.5 ± 0.1	0.9 ± 0.0
	5.8	29.2	30.0	2.0 ± 0.1	1.2 ± 0.1
	5.6	-	18.6 ± 0.1	3.5 ± 0.2	2.2 ± 0.1
MD-MAA40-LT	7.4	N.D [b]	N.D [b]	N.D [b]	N.D [b]
	6	N.D [b]	N.D [b]	N.D [b]	N.D [b]
	5.8	40.6	45.4 ± 0.7	0.5	0.1 ± 0.0
	5.6	21.9	30.9 ± 0.4	1.0	0.3 ± 0.0
MD-MAA_{45}-LT	7.4	N.D [b]	—	—	—
	6	N.D [b]	—	—	—
	5.4	67.1	—	—	—
	5.3	≦20	—	—	—
MD-MAA50-LT	7.4	N.D [b]	N.D [b]	N.D [b]	N.D [b]
	6	N.D [b]	N.D [b]	N.D [b]	N.D [b]
	5.5	43.3	46.1 ± 0.1	0.3	0.09 ± 0.0

[a] Temperature of peak maximum of calorimetric endotherm.

[b] Not detected.

— Not tested.

557

558

559 **Table 3. Diameter of Polymers-Modified Liposomes**

Polymer-modified liposome	Size/nm	Polydispersity
Unmodified	119.7 ± 4.8	0.12
MD-MAA0-LT	117.5 ± 2.7	0.21
MD-MAA20-LT	107.3 ± 2.5	0.13
MD-MAA30-LT	108.1 ± 0.5	0.14
MD-MAA40-LT	106.8 ± 2.5	0.14

560

561

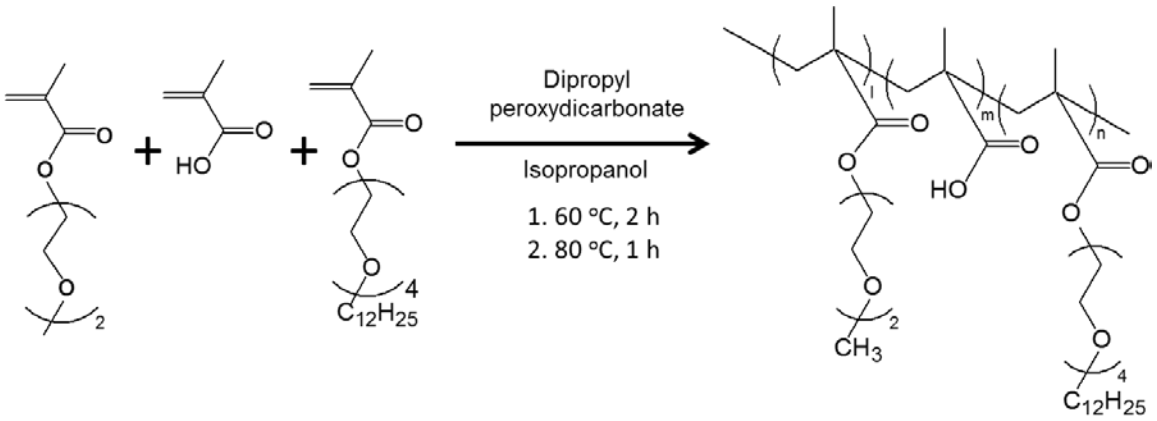

562

563 *Yamazaki et al., Scheme 1.*

564

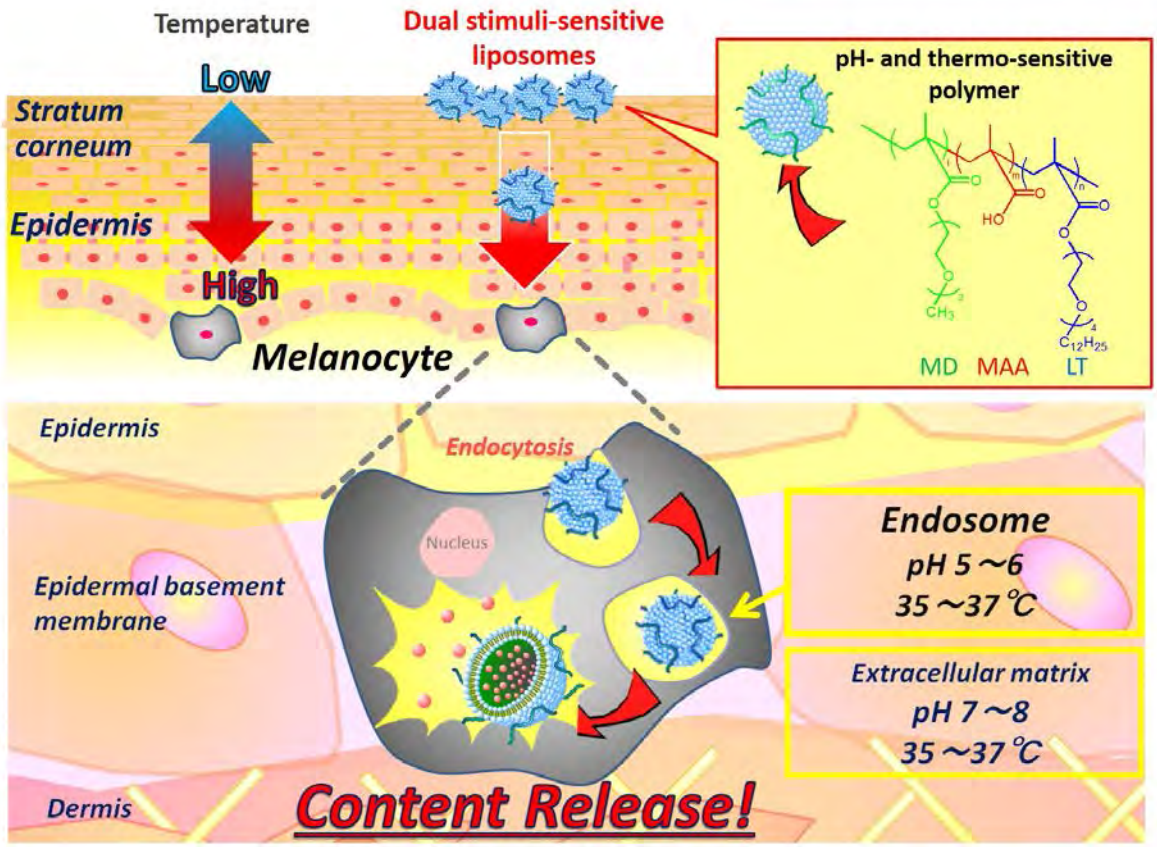

Yamazaki et al., Figure 1.

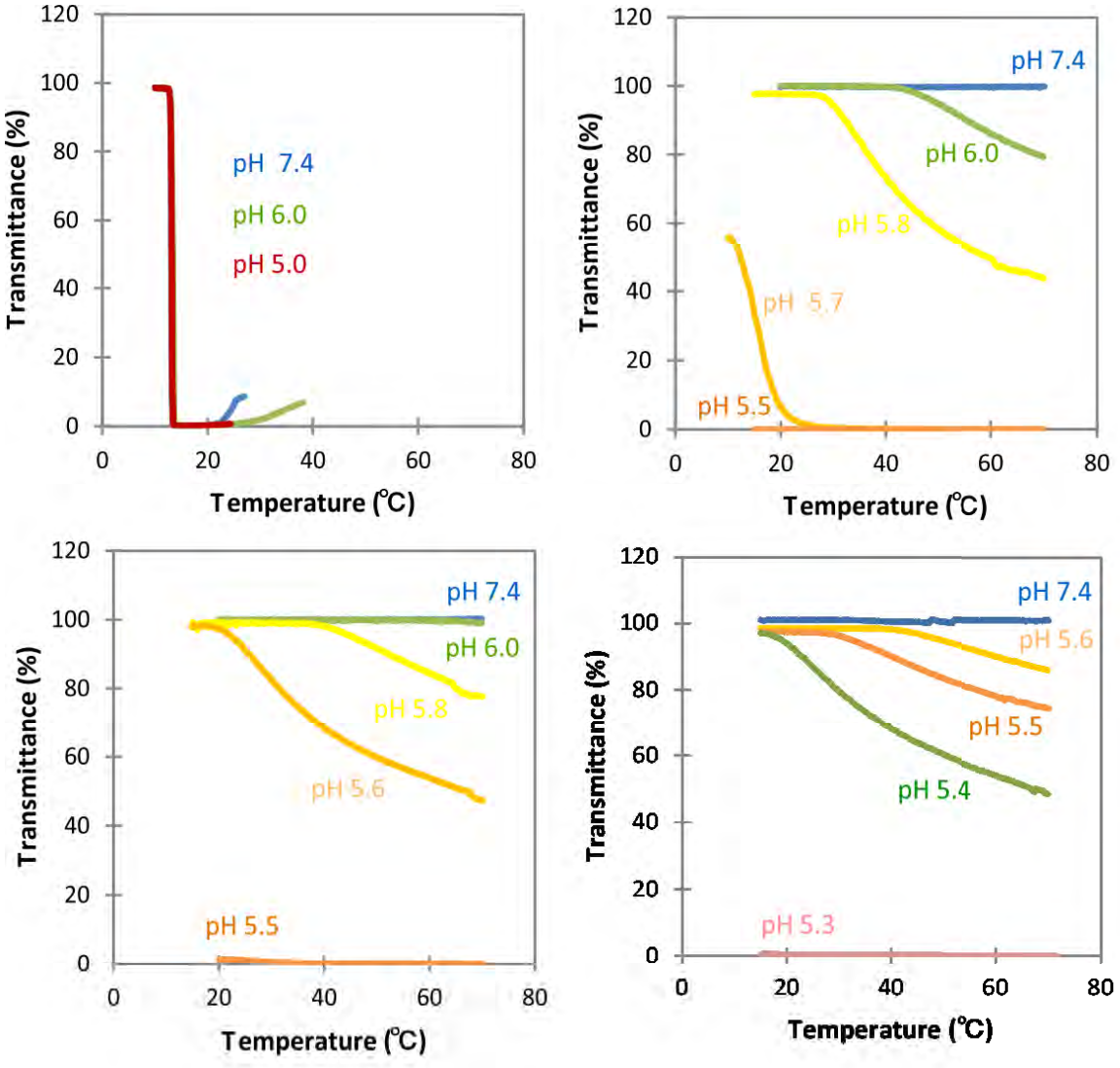

568

569 *Yamazaki et al., Figure 2.*

570

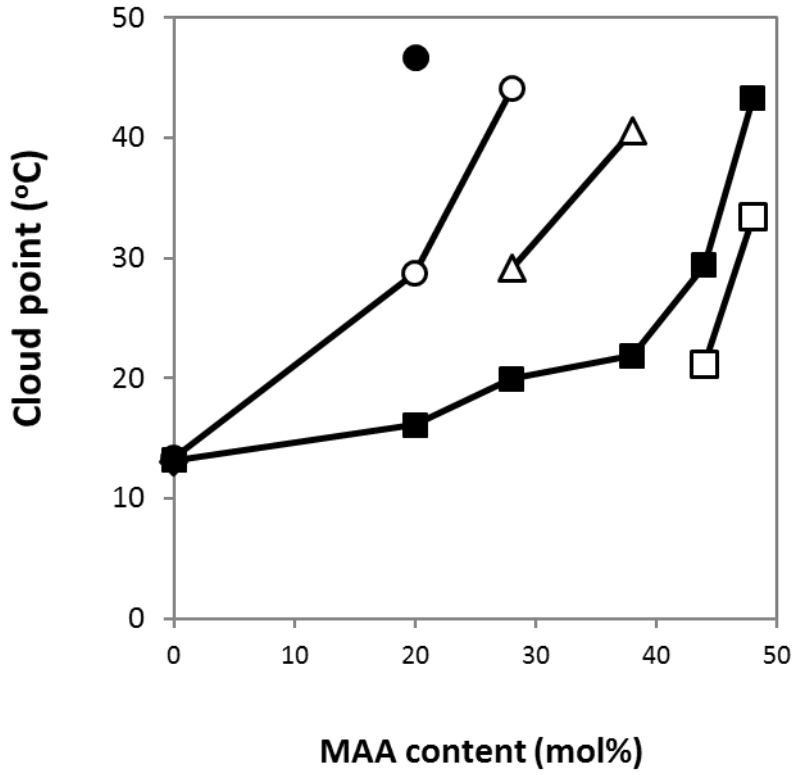

571

572 *Yamazaki et al., Figure 3.*

573

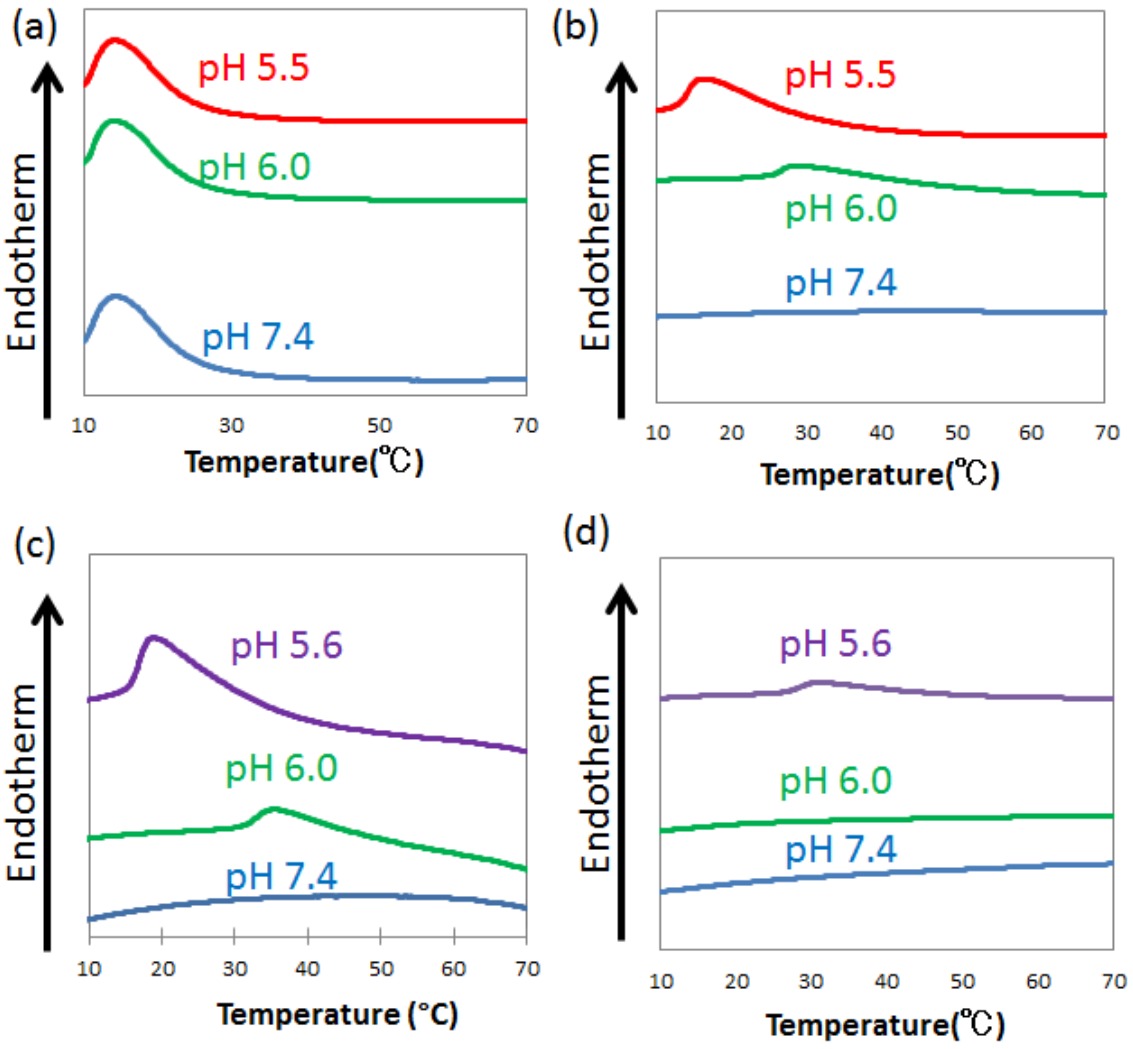

574

575 *Yamazaki et al., Figure 4.*

576

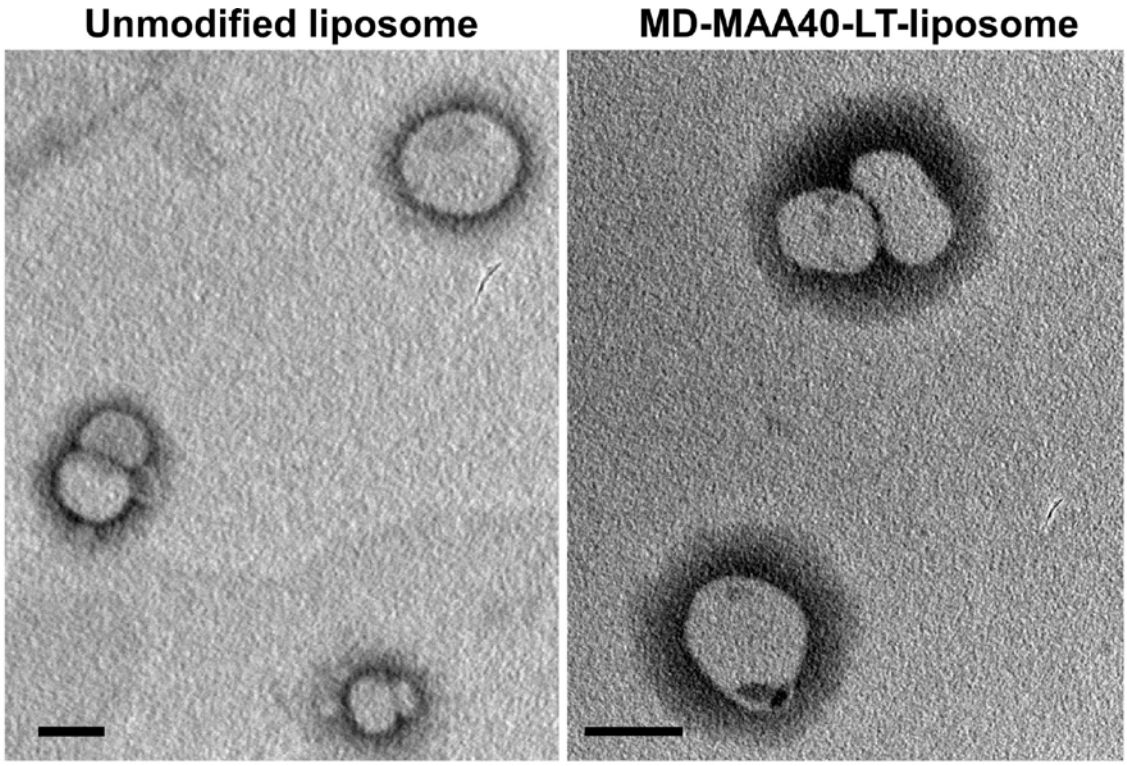

577

578 *Yamazaki et al., Figure 5.*

579

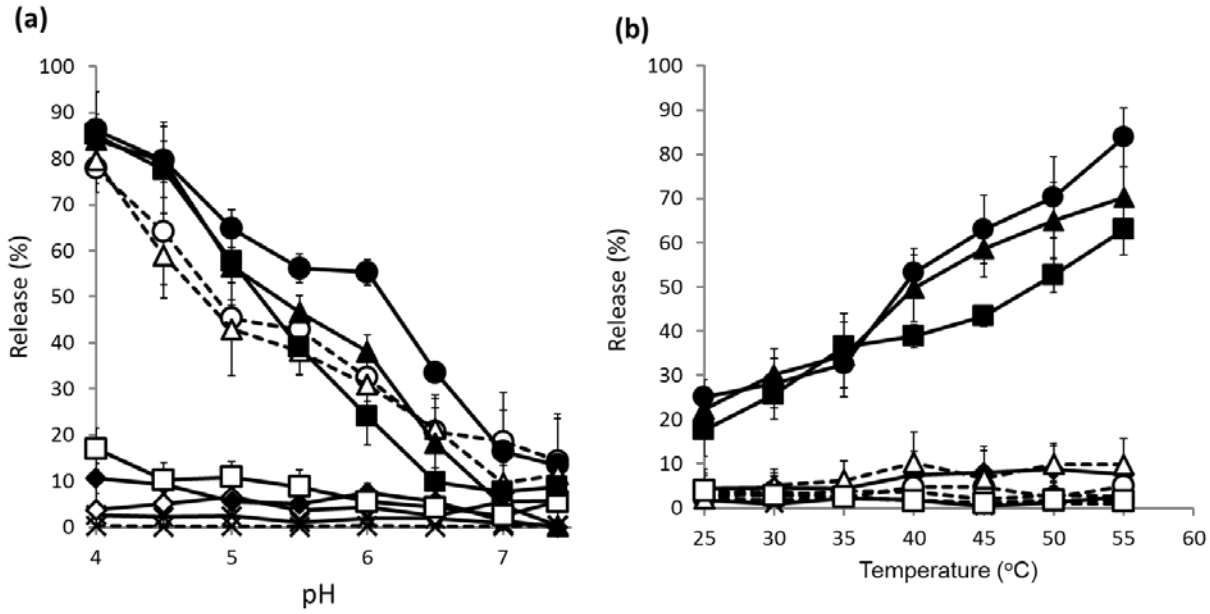

580

581 *Yamazaki et al., Figure 6.*

582

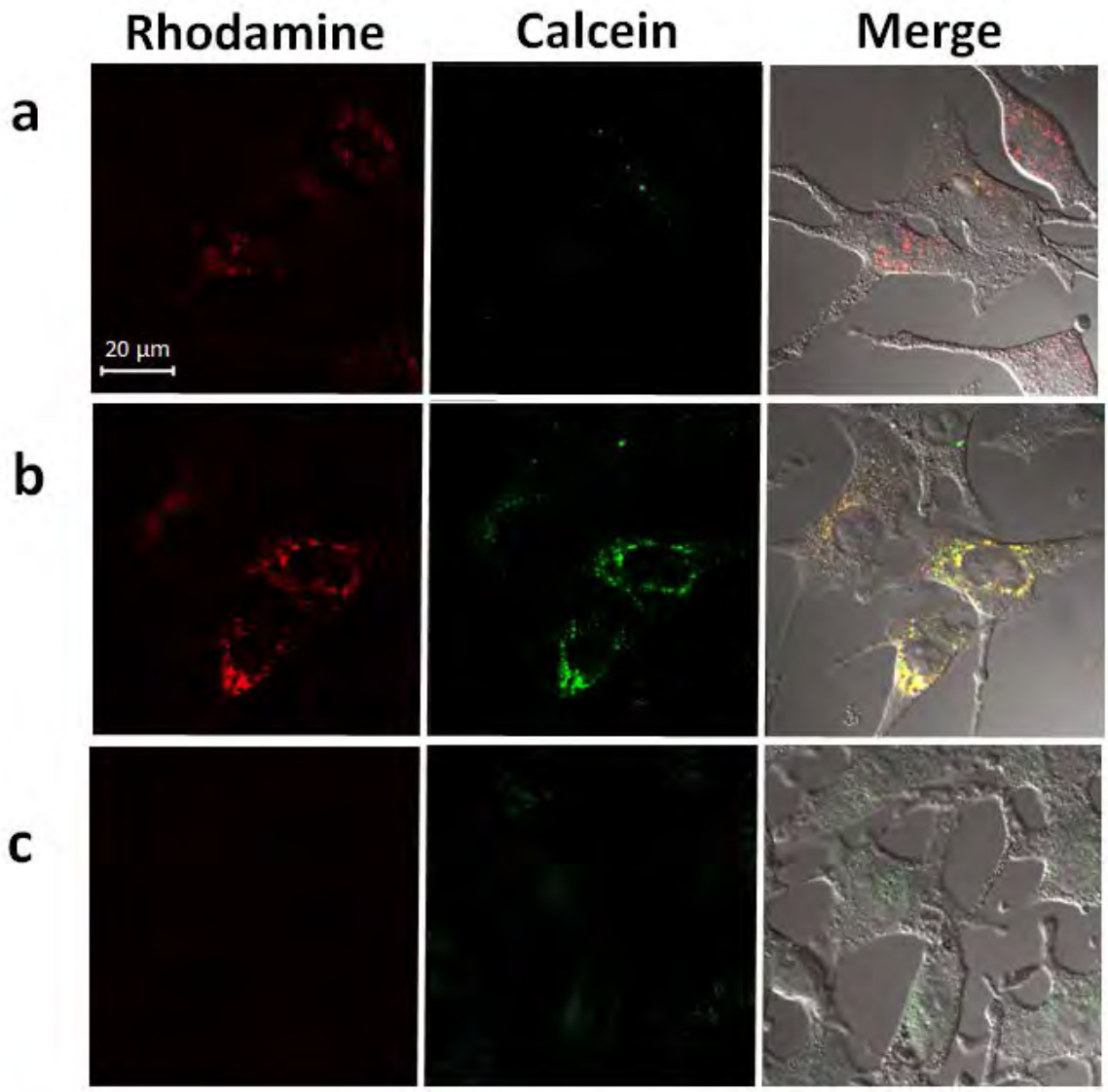

583

584 *Yamazaki et al., Figure 7.*

585

586

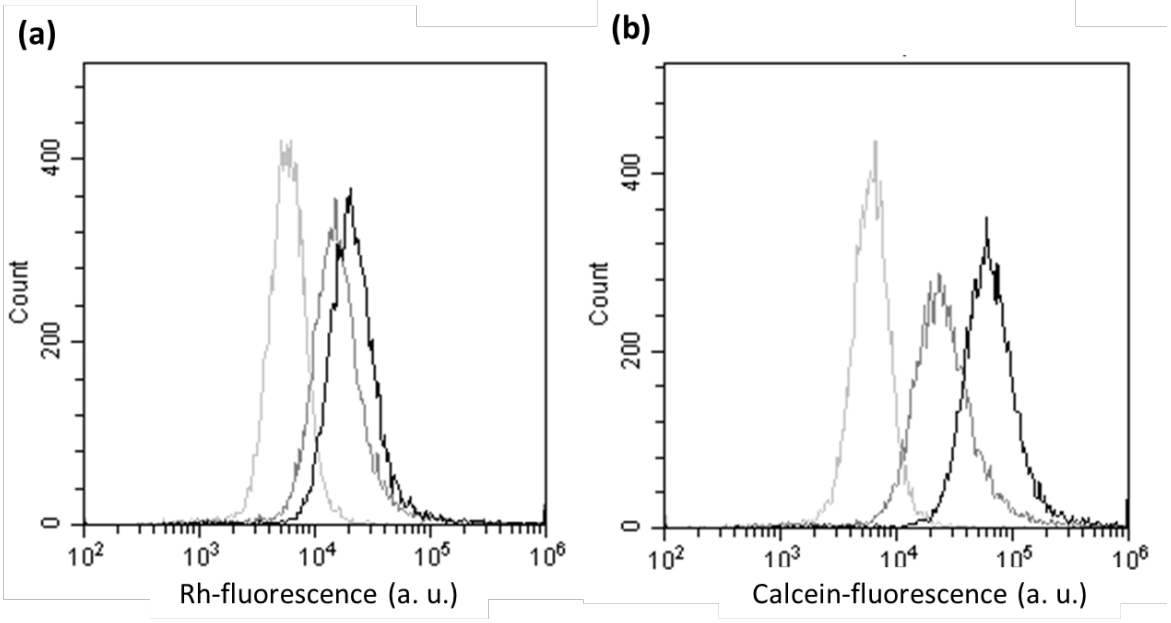

587

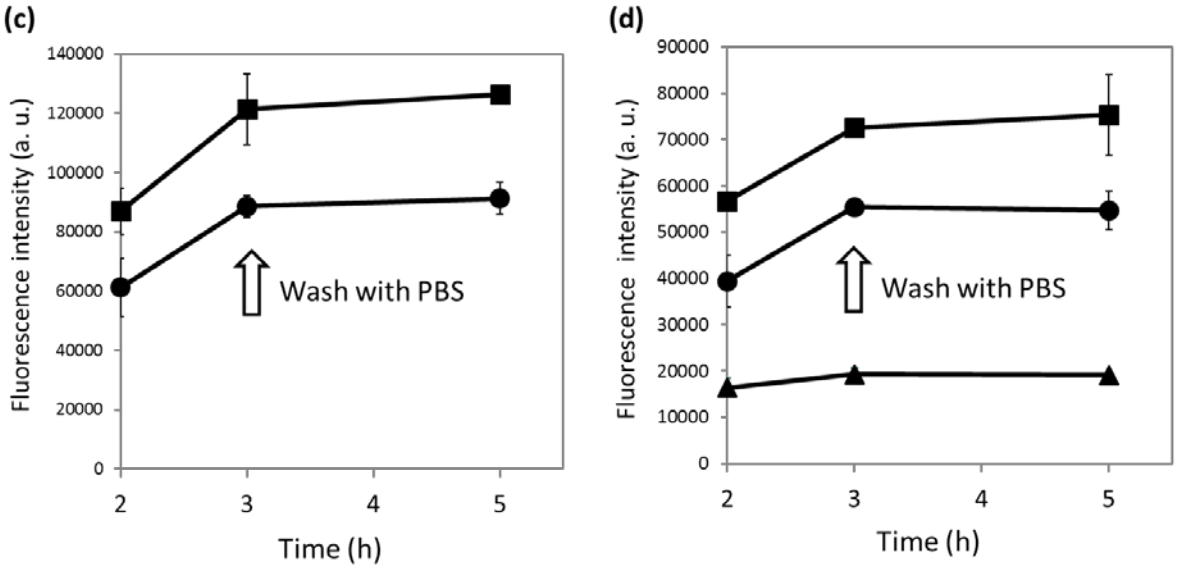

588 *Yamazaki et al., Figure 8.*

589

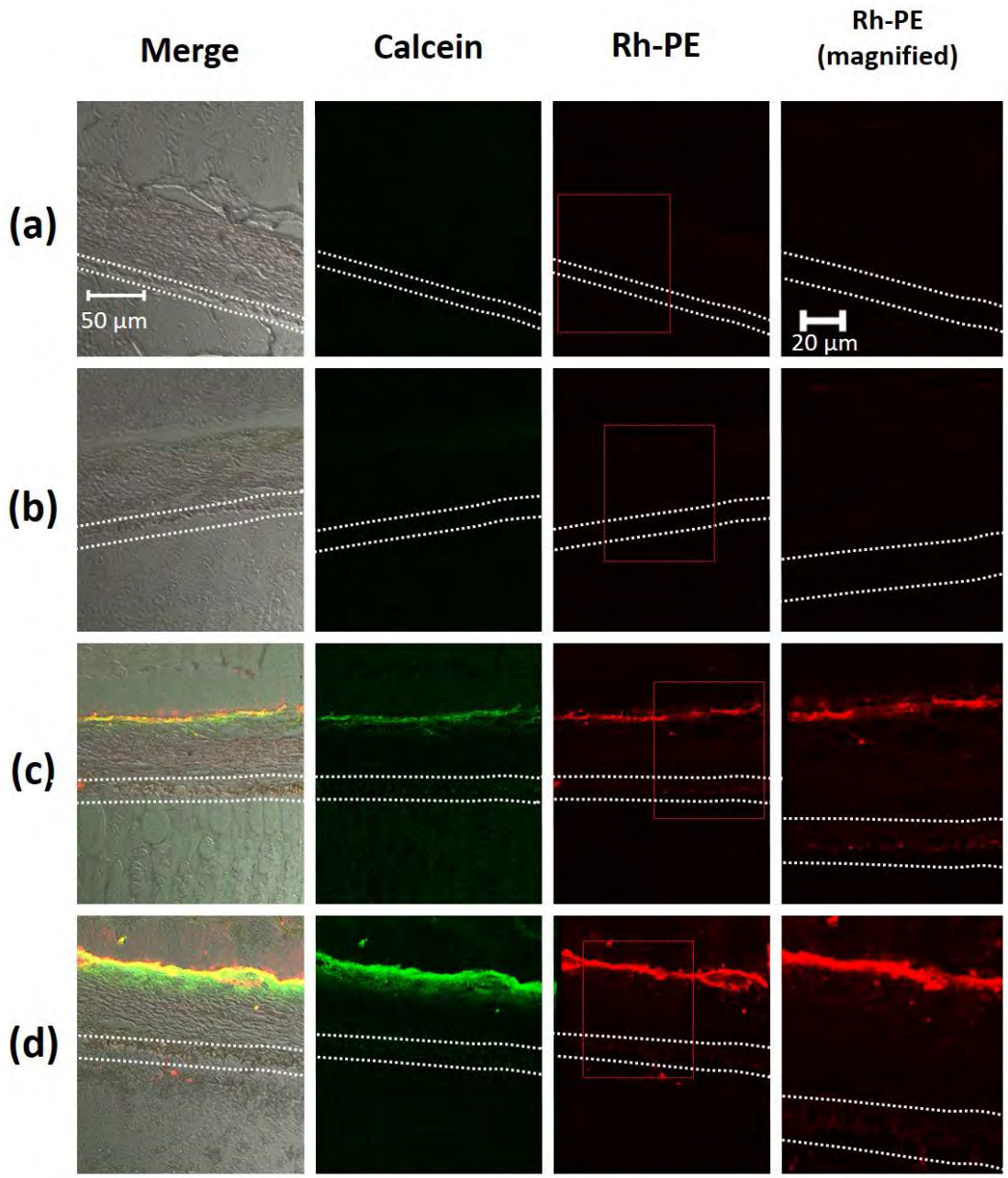

590

591 *Yamazaki et al., Figure 9.*